

Thermopower of Interacting GaAs Bilayer Hole Systems in the Reentrant Insulating Phase Near $\nu = 1$

S. Faniel,^{1,*} E. Tutuc,² E. P. De Poortere,² C. Gustin,¹ A. Vlad,¹ S. Melinte,¹ M. Shayegan,² and V. Bayot¹

¹*Cermin, PCPM and DICE Labs, Université Catholique de Louvain, 1348 Louvain-la-Neuve, Belgium*

²*Department of Electrical Engineering, Princeton University, Princeton, New Jersey 08544, USA*

(Received 30 August 2004; published 2 February 2005)

We report thermopower measurements of interacting GaAs bilayer hole systems. When the carrier densities in the two layers are equal, these systems exhibit a reentrant insulating phase near the quantum Hall state at total filling factor $\nu = 1$. Our data show that, as the temperature is decreased, the thermopower diverges in the insulating phase. This behavior indicates the opening of an energy gap at low temperature, consistent with the formation of a pinned Wigner solid. We extract an energy gap and a Wigner solid melting phase diagram.

DOI: 10.1103/PhysRevLett.94.046802

PACS numbers: 73.40.-c, 71.30.+h, 73.50.Lw

The ground state of two-dimensional (2D) carrier systems has been subject to intensive work over the past decades. The interplay of Coulomb interaction, disorder, and magnetic field B leads to many different ground states [1]. In low-disorder 2D systems, a sufficiently large B is expected to quench the kinetic energy of the carriers, leading to the formation of a Wigner solid (WS) [2]. Experimental evidence has been accumulated for the existence of a WS in both GaAs 2D electron single layers [1–4] around the fractional quantum Hall state at Landau level filling factor $\nu = \frac{1}{5}$ and electron bilayers [5] in the vicinity of total filling factor $\nu = \frac{1}{2}$, as well as in dilute, single-layer, GaAs 2D hole systems [6] near $\nu = \frac{1}{3}$.

Recently, a reentrant insulating phase (IP) was observed in interacting GaAs bilayer hole systems around the many-body quantum Hall state (QHS) at total filling factor $\nu = 1$ [7]. It was suggested in Ref. [7] that this IP signals a bilayer WS, stabilized at such high ν by strong Landau level mixing due to higher effective mass of holes, and by the interlayer Coulomb interaction in the bilayer system. While magnetotransport studies in bilayer systems have intensified in recent years [8], little attention was paid to their thermoelectric properties. Thermopower coefficients are sensitive tools to study the electronic properties of 2D systems, including Si inversion layers [9], SiGe quantum wells [10], and GaAs heterojunctions [11–13]. In particular, as the temperature $T \rightarrow 0$, the diffusion thermopower is expected to vanish as $T^{1/3}$ for a mobility gap or diverge as T^{-1} in the presence of an energy gap [14].

We study here the thermopower of interacting GaAs bilayer hole systems around $\nu = 1$. When the hole densities in the two layers are equal, at filling factors near $\nu = 1$, our measurements show that the diffusion thermopower diverges as T^{-1} when the temperature is lowered below ~ 100 mK. This behavior corroborates the magnetotransport [7] and the nonlinear I - V results. The T dependence of the thermopower indicates the opening of an energy gap, consistent with the formation of a pinned,

bilayer WS near the QHS at $\nu = 1$, and allows us to extract a phase diagram for the WS melting.

The samples we have studied are Si modulation-doped GaAs bilayer hole systems grown by molecular beam epitaxy on undoped GaAs (311)A wafers. The two samples consist of two 15 nm wide GaAs quantum wells separated by an AlAs barrier with a thickness of 11 nm (sample A) and 7.5 nm (sample B). The width of the AlAs barrier and the large effective mass of the holes assure a weak interlayer tunneling [15]. Two 8×2 mm² rectangular pieces of wafer were cut with their length along the $[01\bar{1}]$ (sample A) and $[\bar{2}33]$ (sample B) crystallographic directions. On both specimens, we patterned 400 μ m wide Hall bars in order to reduce density inhomogeneities; the distance between the voltage probes along the Hall bar is 1.2 mm. Ohmic contacts were made to both layers. A back-gate was used to tune the charge distribution of the two layers. The charge imbalance is denoted by $\Delta p = (p_T - p_B)/2$, where p_B and p_T are the hole densities of the bottom and the top layer, respectively. For balanced charge distributions ($\Delta p = 0$), the total hole density for both samples is close to $p = 5 \times 10^{11}$ cm⁻² [16]. Our experimental setup for thermopower measurements is described in Ref. [12]. One end of each sample was mounted onto the cold finger of a dilution refrigerator, while a strain gauge, used as heater, was glued on the other end using General Electric varnish. To measure the longitudinal thermopower S_{xx} , a thermal gradient was created along the sample by applying a sine wave current at a frequency $f = 1.3$ Hz through the heater and measuring, via a lock-in amplifier, the voltage signal at $2f$ between two contacts on the same edge of the Hall bar. The temperature gradient was determined using two carbon paint thermometers deposited on the sample's surface, and was kept below 10% of the mean T .

We first summarize the magnetotransport results for our samples. In Fig. 1, we illustrate for sample A the longitudinal resistivity ρ_{xx} as a function of B at low T . Consistent with the sample's extremely small interlayer tunneling

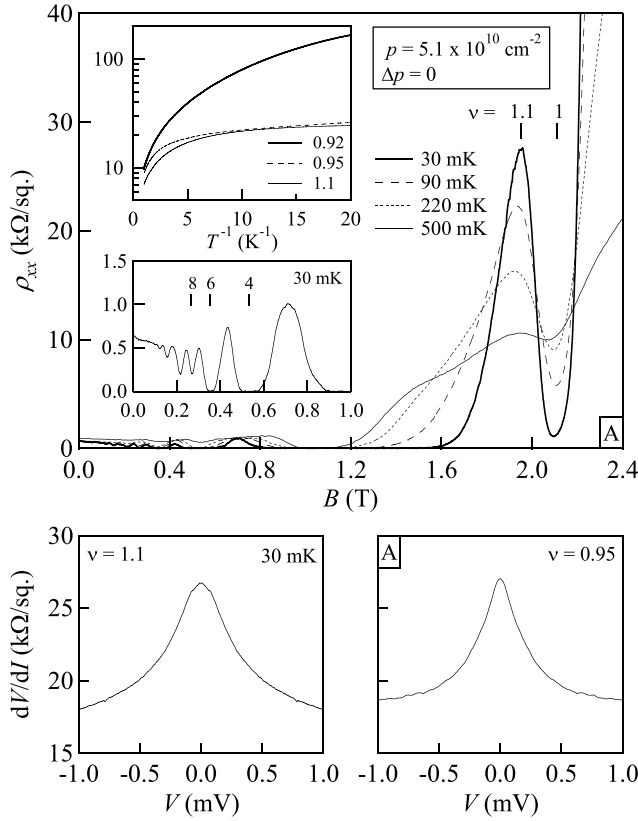


FIG. 1. Upper panel: longitudinal resistivity ρ_{xx} as a function of B at the indicated temperatures for sample A at a total density $p = 5.1 \times 10^{11} \text{ cm}^{-2}$. For the data in the figure, the densities of the individual layers are equal ($\Delta p = 0$). Top inset: the T dependence of ρ_{xx} at $\nu = 0.92, 0.95$, and 1.1 . Bottom inset: a magnified view of the low- B ρ_{xx} trace at 30 mK. Lower panels: differential resistance in the insulating phase of sample A as a function of the dc bias for $\nu = 1.1$ (left panel) and 0.95 (right panel) at 30 mK.

[15], at low B the ρ_{xx} trace exhibits minima only at even integer fillings $\nu = 2, 4, 6$, etc. The strong interlayer interaction, however, leads to a many-body QHS at $\nu = 1$ [8], flanked by reentrant IP's [7]. The measured QHS excitation gaps $^1\Delta$, extracted from the T dependence of ρ_{xx} at $\nu = 1$, are 0.13 and 0.67 K, respectively; the larger $^1\Delta$ for sample B is consistent with its smaller d/l_B ratio [16]. The T dependence of ρ_{xx} at $\nu = 0.92, 0.95$, and 1.1 is displayed in the top inset to Fig. 1, revealing the insulating behavior at these fillings. Finally, in the bottom panels of Fig. 1 we show I - V characteristics at filling factors near $\nu = 1$ for sample A, exhibiting a strongly nonlinear behavior. We have observed qualitatively similar I - V curves for sample B also. These nonlinear data are similar to previous measurements in the IP near $\nu = \frac{1}{3}$ in single-layer GaAs 2D hole systems [6].

Before discussing our S_{xx} data, we briefly review the essential concepts for understanding thermopower data in 2D carrier systems [17]. In general, S_{xx} consists of two

additive contributions: the phonon-drag thermopower S_{xx}^g and the diffusion thermopower S_{xx}^d . In GaAs-based heterostructures, the former is known to be dominant for $T \gtrsim 200$ mK, while the latter provides the main contribution at lower temperatures ($T \lesssim 100$ mK). The phonon-drag thermopower is given by $S_{xx}^g = \frac{C}{3pe} \frac{\Lambda}{v_s \tau_{ph}}$, where C is the specific heat, Λ is the phonon mean free path, e is the electron charge, v_s is the sound velocity, and τ_{ph} is the phonon momentum relaxation time due to scattering with holes only [17]. The diffusion thermopower, on the other hand, measures the heat or the entropy per carrier and is sensitive to the density of states at the Fermi level. In particular, for a 2D insulating system, S_{xx}^d can distinguish between a mobility gap and an energy gap. In the first case, S_{xx}^d should vanish at low T as $S_{xx}^d \propto T^{1/3}$, while for the second case—when an energy gap E_g separates the ground state from its excitations— S_{xx}^d is expected to diverge at low T as [14,18,19]

$$S_{xx}^d \cong \frac{k_B}{2e} \frac{E_g}{k_B} T^{-1}. \quad (1)$$

Hence, S_{xx}^d is a unique probe of the ground state of 2D systems as it can critically test if the IP results from the strong localization of the carriers (mobility gap) or from the formation of a pinned WS (energy gap).

We now present the result of our S_{xx} measurements, summarized in Figs. 2 and 3, and consider first the phonon-drag regime. Figure 2 shows S_{xx} vs B traces for sample A at various temperatures. The curves at $T = 285, 310$, and 365 mK, where the phonon drag is dominant, are displayed in the Fig. 2 inset. Similar to ρ_{xx} data, we observe minima at even filling factors ($\nu = 2, 4$, and 6) and at $\nu = 1$ consistent with a vanishing density of states at the Fermi level [17]. In the phonon-drag regime, a dramatic

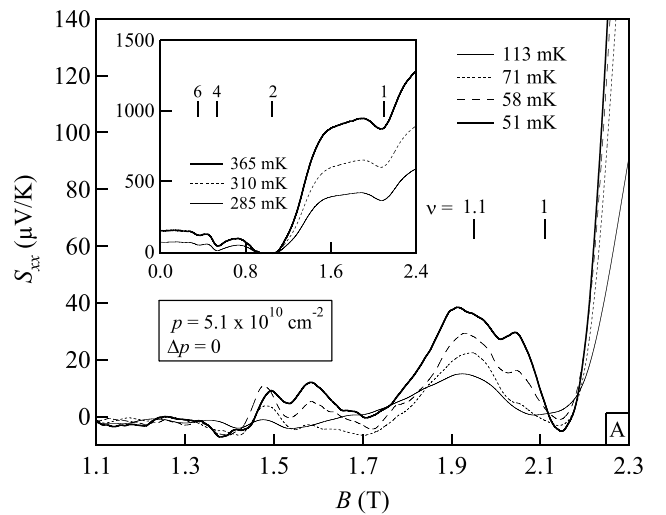


FIG. 2. S_{xx} as a function of B at four temperatures below 120 mK for sample A. Inset: S_{xx} vs B is displayed at $T = 285, 310$, and 365 mK in the phonon-drag regime.

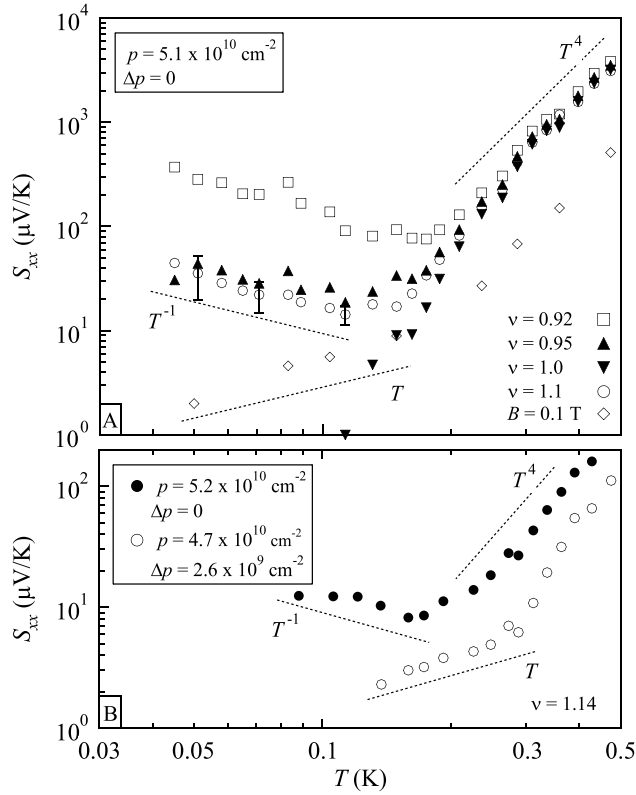


FIG. 3. Top panel (sample A): T dependence of S_{xx} at different filling factors when the bilayer is balanced. Bottom panel (sample B): T dependence of S_{xx} at $\nu = 1.14$ for balanced (\bullet) and imbalanced (\circ) charge distributions. The dotted lines indicate various T dependencies. The error bars are given by the noise of the lock-in amplifier, the magnitude of the applied thermal gradient, and the accuracy of the thermometers' calibration.

decrease of S_{xx} is found in the entire investigated B range as T diminishes. This is clearly indicated by the T evolution of S_{xx} at various fillings shown in Fig. 3 for both samples. In the top panel of Fig. 3, S_{xx} vs T is displayed for sample A at $\nu = 1.1, 1, 0.95, 0.92$ and for $B = 0.1$ T when the bilayer system is balanced. In the bottom panel of the figure, we show S_{xx} vs T for sample B. Data points are presented at $\nu = 1.14$ for a balanced and a slightly imbalanced charge distribution. At high T , $S_{xx} \cong S_{xx}^g$ follows the well known T^4 law [20] for all the experimental configurations shown in Fig. 3 [21].

At low temperatures, where the thermopower is dominated by the diffusion contribution, S_{xx} increases with decreasing T in the IP's reentrant around $\nu = 1$. This main result of our work is illustrated in Fig. 2 by the S_{xx} vs B traces at $T = 113, 71, 58,$ and 51 mK [22]. The divergence of S_{xx} at low T in the IP is further illustrated in Fig. 3. Focusing on the data shown in the top panel of Fig. 3, we observe that at $\nu = 1$, S_{xx} rapidly approaches zero as expected for a QHS with no entropy [14], and S_{xx} at $B = 0.1$ T is proportional to T below 200 mK as expected for a diffusion-dominated thermopower in a metallic sys-

tem. However, at $\nu = 1.1, 0.95,$ and 0.92 , $S_{xx} \propto T^{-1}$ as $T \rightarrow 0$. This divergence of S_{xx} in the reentrant IP's at very low T indicates the opening of an energy gap and suggests the formation of a pinned bilayer WS near $\nu = 1$.

Data for sample B exhibit qualitatively the same behavior. In the lower panel of Fig. 3 we show S_{xx} vs T data for sample B at $\nu = 1.14$ where this sample's magnetotransport data reveal an IP. The S_{xx} data show a divergence at low T when the bilayer system is balanced (closed circles, $\Delta p = 0$). In the same panel we also show data (open circles, $\Delta p = 2.6 \times 10^9 \text{ cm}^{-2}$) for sample B when charge distribution is imbalanced, i.e., when charge is removed from the bottom layer via the application of positive back-gate bias. For the imbalanced state, S_{xx} at $\nu = 1.14$ turns from a T^{-1} to an approximately linear temperature dependence. This observation is in agreement with magnetotransport results showing that the reentrant IP disappears for small charge imbalance between the two layers [7]. We note that the strengthening of the $\nu = 1$ QHS when Δp increases, seen in the magnetotransport [7], is also observed in thermopower measurements. In other words, the filling factor range around $\nu = 1$ where $S_{xx} \rightarrow 0$ as $T \rightarrow 0$ extends when charge is transferred from one layer to the other (data not shown here).

We now turn to a more quantitative discussion of our thermopower data. From the T dependence of S_{xx} , shown in Fig. 3 and the inset to Fig. 4, we can extract a phase diagram for the WS melting. To estimate the melting temperature T_m , we assume that the solid-to-liquid transition occurs when S_{xx} starts to rise as T is lowered. As illustrated in the inset to Fig. 4 for $\nu = 0.93$, we have fitted at fixed filling factors the phonon-drag thermopower with a

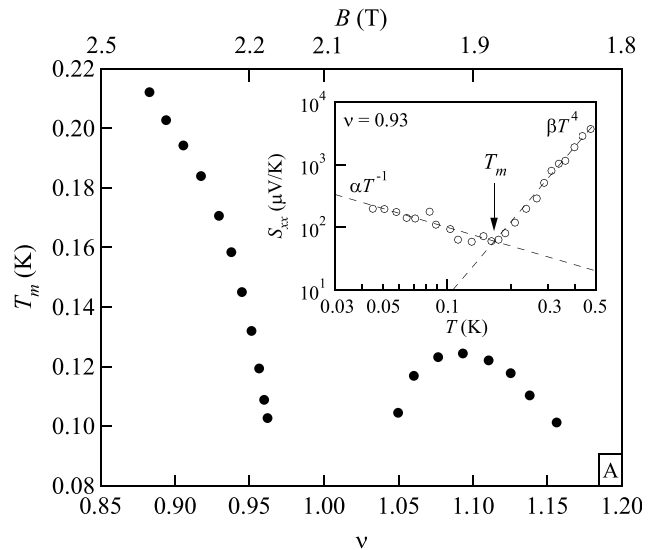


FIG. 4. Evolution of the melting temperature T_m as a function of ν of the pinned, bilayer WS in sample A. The top axis shows the corresponding magnetic fields. Inset: T_m is extracted from the T dependence of S_{xx} by assuming that the rise in S_{xx} signals the melting of the WS.

T^4 law for $T \geq 200$ mK and the diffusion thermopower with a T^{-1} law for $T \leq 100$ mK. The intersection of these two fits determines $T_m(\nu)$. In Fig. 4, the T_m vs ν phase diagram is shown for sample A. The reentrant behavior of the IP is illustrated by the evolution of T_m ; T_m is finite in a small filling range centered near $\nu = 1.1$ and at $\nu \geq 0.95$, but is vanishingly small near $\nu = 1$ ($B = 2.1$ T) where the quantum Hall ground state is present. The magnitude of the estimated T_m in our sample is similar to the reported values of the WS melting temperature in single-layer 2D hole [12] and electron [3,23] systems around $\nu = \frac{1}{3}$ and $\frac{1}{5}$, respectively. Using Eq. (1) and the $S_{xx} = \alpha T^{-1}$ fit to the diffusion regime, an estimate of the energy gap associated with the pinned WS can be made when $E_g \gg k_B T$ [12]. This energy gap likely corresponds to the creation energy of thermally activated defects (such as bound pairs of dislocations), which may be responsible for electrical conduction in the pinned WS [24]. For example, at $\nu = 0.92$, $E_g/k_B = 0.34$ K in sample A. This value is of the same order of magnitude as the activation energy $E_A/k_B = 0.15$ K determined from fitting ρ_{xx} in the low- T range to $\ln(\rho_{xx}) \propto E_A/2k_B T$, and compares well with the WS melting temperature $T_m = 0.18$ K at this filling.

To conclude, we have measured the thermopower of interacting GaAs bilayer hole systems around $\nu = 1$. At very low T , when the diffusion thermopower dominates, S_{xx} diverges in the IP's reentrant around $\nu = 1$. This behavior indicates the opening of an energy gap and the presence of a pinned bilayer WS. We have interpreted our thermopower data in terms of a WS melting and extracted a T_m vs ν phase diagram.

The work was supported by the DOE and the NSF, the von Humboldt Foundation, "Actions de recherches concertées (ARC) - Communauté française de Belgique," and by the Belgian Science Policy through the Interuniversity Attraction Pole Program PAI (P5/1/1). S.F. acknowledges financial support from the F.R.I.A. and S.M. from the F.N.R.S.

*Electronic address: faniel@pcpm.ucl.ac.be

- [1] For a review, see *Perspectives in Quantum Hall Effects*, edited by S. Das Sarma and A. Pinczuk (Wiley, New York, 1997).
- [2] See reviews by H. Fertig and by M. Shayegan in Ref. [1].
- [3] V. J. Goldman *et al.*, Phys. Rev. Lett. **65**, 2189 (1990).
- [4] H. W. Jiang *et al.*, Phys. Rev. Lett. **65**, 633 (1990).
- [5] H. C. Manoharan *et al.*, Phys. Rev. Lett. **77**, 1813 (1996).
- [6] M. B. Santos *et al.*, Phys. Rev. Lett. **68**, 1188 (1992).
- [7] E. Tutuc *et al.*, Phys. Rev. Lett. **91**, 076802 (2003).
- [8] For recent work, see M. Kellogg *et al.*, Phys. Rev. Lett. **90**, 246801 (2003) and references therein.

- [9] B. L. Gallagher *et al.*, J. Phys. Condens. Matter **2**, 755 (1990); R. Fletcher *et al.*, Phys. Rev. B **56**, 12422 (1997).
- [10] C. Possanzini *et al.*, Phys. Rev. Lett. **90**, 176601 (2003).
- [11] C. Ruf *et al.*, Superlattices Microstruct. **6**, 175 (1989); U. Zeitler *et al.*, Phys. Rev. B **47**, R16008 (1993); L. Moldovan *et al.*, Phys. Rev. Lett. **85**, 4369 (2000).
- [12] V. Bayot *et al.*, Europhys. Lett. **25**, 613 (1994).
- [13] R. J. Hyndman *et al.*, Physica B (Amsterdam) **249-251**, 745 (1998).
- [14] P. M. Chaikin, in *Organic Superconductivity*, edited by V. Z. Kresin and W. A. Little (Plenum, New York, 1990), p. 101.
- [15] A simple band calculation yields a tunneling energy Δ_{SAS} less than $1 \mu\text{V}$ for the bilayer systems studied here.
- [16] The ratio of intralayer and interlayer energies, given by d/l_B where d is the interlayer distance and l_B is the magnetic length at $\nu = 1$, is 1.47 for sample A and 1.29 for sample B.
- [17] See, e.g., B. L. Gallagher and P. N. Butcher, in *Handbook of Semiconductors*, edited by P. T. Landsberg (Elsevier, New York, 1992), Vol. 1, p. 721.
- [18] J. M. Ziman, *Electrons and Phonons* (Oxford University Press, New York, 1972).
- [19] It is useful to describe $S = j_Q/(j_E T)$, where j_Q and j_E are the microscopic heat and electric currents, respectively. If the drift velocity of charge carriers is v_d and their mobility μ , then $j_E = p e v_d$, $j_Q = Q v_d$, and $\rho = 1/(p e \mu)$. When the charge carriers are excited across an energy gap E_g , the heat current is $j_Q = \frac{E_g}{2} p v_d$ as the characteristic heat of carriers is the difference between the band edge energy and the chemical potential, i.e., $Q \cong \frac{E_g}{2}$. The thermopower is then $\cong \frac{(k_B)}{2e} \left(\frac{E_g}{k_B T} \right)$ and diverges as $T \rightarrow 0$. Therefore the microscopic reason of thermopower's divergence is that the carriers carry a minimum amount of heat $E_g/2$, while the divergence of the resistivity is due to the fact that less and less carriers are excited across the gap as $T \rightarrow 0$.
- [20] S. K. Lyo, Phys. Rev. B **38**, R6345 (1988).
- [21] We note that S_{xx}^g , for $T > 200$ mK, is one order of magnitude larger in sample A than in sample B. The difference likely results from different values of Λ , which depends on the specimens' macroscopic properties such as thickness and surface roughness [see V. Bayot, E. Grivei, H. C. Manoharan, X. Ying, and M. Shayegan, Phys. Rev. B **52**, R8621 (1995) and Ref. [17]].
- [22] In the field range $1.3 < B < 1.7$ T, we observe a weak (nonzero), oscillating S_{xx} signal. We do not know the origin of these features. We speculate that they may be signaling the presence of fractional QHS's (e.g., at $\nu = \frac{4}{3}$), and a competition between such states and the engulfing IP. We note that we observe some of these features (e.g., an S_{xx} minimum near $\nu = \frac{4}{3}$) in some S_{xx} vs B traces of sample B also. Note that, interestingly, ρ_{xx} in this field range is rather featureless and shows a deep minimum ($\rho_{xx} > 0$).
- [23] M. A. Paalanen *et al.*, Phys. Rev. B **45**, R13784 (1992).
- [24] K. Esfarjani *et al.*, Phys. Rev. B **46**, 4638 (1992) and references therein.